IEEE Access
Multidisciplinary | Rapid Review | Open Access Journal

SPECIAL SECTION ON THEORY, ALGORITHMS, AND APPLICATIONS OF SPARSE RECOVERY

Received June 5, 2018, accepted July 2, 2018, date of publication July 5, 2018, date of current version July 30, 2018.

Digital Object Identifier 10.1109/ACCESS.2018.2853180

High-Speed Target Detection Algorithm Based on Sparse Fourier Transform

CUNSUO PANG[1,2], SHENGHENG LIU[3], (Member, IEEE), AND YAN HAN[1,2]

[1]National Key Laboratory of Electronic Measurement Technology, North University of China, Taiyuan 030051, China
[2]Shanxi Key Laboratory of Information Detection and Processing, Taiyuan 030051, China
[3]School of Engineering, The University of Edinburgh, Edinburgh EH9 3JL, U.K.

Corresponding author: Cunsuo Pang (pangcunsuo@126.com)

This work was supported by the Natural Science Foundation of Shanxi Province of China under Grant 201701D121064.

ABSTRACT Radar detection of high-speed targets suffers from range walks during the integration time. Methods in current use for mitigating range walks are beset by high computational complexity therein that hinders practical real-time processing. In this context, we exploit the sparsity of the target echo in the transform domain and propose an efficient range walk mitigation algorithm based on sparse Fourier transform (SFT). Concretely, the input long echo sequence is first divided into short overlapped segments with an SFT bucket structure. Then, speed compensation is performed to the short segments, which involves less complex multiplications. Subsequently, SFT is employed which efficiently obtains the Fourier transform of the long sequence such that the range alignment of the multi-pulse echo is accomplished. As such, the proposed SFT-based algorithm significantly reduces the amount of complex multiplications required in speed compensation and long sequence transform, and thus substantially improves the computational efficiency. In this paper, the selection of the window function and the length of segments are examined for their influence on the detection performance with different signal-to-noise ratios. The superiorities of the proposed algorithm in both detection performance and computational efficiency are demonstrated by numerical experiments. The proposed algorithm can potentially find applications in other radar systems such as synthetic aperture radars, inverse synthetic aperture radars, and so on where echo range walk is also encountered.

INDEX TERMS High-speed target, range walk, sparse Fourier transform (SFT), computational complexity.

I. INTRODUCTION

Classical moving target detection (MTD) methods assume that a target does not walk in a certain range bin within the integration time. However, this assumption does not hold for weak and high-speed targets, for the long integration time and the high speed conspire to induce considerable range bin walk. This situation has a negative impact on the integration gain of the MTD methods and consequently leads to a lowered detection probability [1]–[3]. Commonly used methods to address such problem associated with multi-pulse echo include envelope shift, keystone, Radon transform, Hough transform, Radon-Fourier transform, maximum likelihood method, and their variants [2]–[15]. Although these methods indeed improve the target detection performance, they share a common drawback as their overall computational efficiency is not sufficiently high. More specifically, when the target speed is high and unknown, the number of required speed compensation operations increases dramatically. In addition, when the target range is large, the processing length of the echo signal increases to such a degree that the fast Fourier transform (FFT) operation load becomes unaffordable, making it difficult to meet the system real-time requirement. In the light of this, [16], [17] proposed a scaled inverse Fourier transform (SCIFT)-based method to achieve fast estimation of an unknown speed. This method, relying mostly on cross-correlation technique to introduce a third variable τ_m, converts the relationship between the fast and slow time signals into that between the fast time signal and τ_m. Next, scaling is used to remove the coupling between the fast time signal and τ_m, and the FFT technique is used to estimate the speed. The resulting runtime is reduced by 4 to 5 times compared to the keystone transform-based method [9]. However, with this method, the utilization ratio of the available samples is decreased by 50% and, at false alarm probability $p_f = 10^{-6}$, the signal-to-noise ratio (SNR) drops by about 5 dB relative to keystone transform, making it unsuitable for

weak target detection. Reference [18] adopted the compressive sensing technique to improve the detection efficiency of high-speed targets. This method, however, has limited application as it involves a complicated process of generating the sparse matrix of the target echo. Reference [19]–[24] put forward the sparse Fourier transform (SFT) method for sparse signals in the frequency domain. Such method is more efficient than the FFT-based method when computing the spectra of large-scale signals. Reference [23] and [24] utilized the SFT method and achieved fast detection of high-dynamic signals and high-acceleration targets. Taking into account that long-range, high-speed and weak target signals are characterized by larger length and sparsity in the transform domain, this paper employs SFT to accelerate the speed compensation and spectrum computation of high-speed targets.

The remainder of this paper is structured as follows. Section II provides a brief overview of range walk and its relationship with various parameters. The influence of range walk on the echo integration gain and state-of-the-art compensation algorithm is also addressed. Section III presents the proposed SFT-based range walk compensation method, where signal bucketing length and speed compensation factor are also discussed. Numerical experiment results and their corresponding analyses are given in Section IV. Section V is dedicated to summary and future work.

II. PRELIMINARY

A. RANGE WALK

With the effect of noise neglected, [12] gives what results from MTD processing of high-speed target echo. The result is approximated by:

$$z(\hat{t},f) \approx A_0\sqrt{D}\Big|\sum_{n=0}^{N-1}\mathrm{sinc}\left[\pi B_s\left(\hat{t}-\tau_0+\beta_0 nT+\frac{f_d}{\mu}\right)\right] \bullet \exp\left(-j\pi\frac{f_d^2}{\mu}\right)\exp\left(j\pi f_d\left(\hat{t}+\tau_0-\beta_0 nT+\tfrac{f_d}{\mu}\right)\right) \times \exp\left(j2\pi f_d nT\right)\Big| \quad (1)$$

where, A_0 is the target amplitude, D is the product of time-width and bandwidth, $\tau_0 = 2R_0/c$ is the initial delay of the target, $\beta_0 = 2v_0/c$ is the time delay variation rate of the target, $f_d = 2v_0/\lambda$ is the Doppler frequency of the target, $\lambda = c/f_c$ is the emission signal wavelength, B_s is the signal bandwidth, T is the pulse repetition period, μ is the FM slope of the transmitted pulse signal, f_c is the carrier frequency, c is the electromagnetic wave speed, v_0 is the initial speed of the target, R_0 is the initial range between the radar and the target, $\hat{t}$ is the fast time domain, and $n = 0, \ldots, N-1$, with N being the number of pulses.

From (1), the effect of speed on the accumulated energy of the echo can be written as:

$$z(\hat{t},f) \approx A_0\sqrt{D}\Big|\sum_{n=0}^{N-1}\mathrm{sinc}\left[\pi B\left(\hat{t}-\tau_0+\beta_0 nT+\frac{f_d}{\mu}\right)\right]\Big| \quad (2)$$

From (2), we know that the envelope range walk time delay $\Delta\tau$ of the nth target echo relative to the 1st target echo is:

$$\Delta\tau \approx \beta_0 nT \quad (3)$$

From (3) we find that the cross-range bin number R_L of the target echo envelope may be written as:

$$R_L = c\Delta\tau/2\Delta R = \frac{\beta_0 cnT}{2}/\Delta R \quad (4)$$

where, $\Delta R = c/2B$ is the radar range resolution. Equation (3) shows that R_L is proportional to speed, integration time, and signal bandwidth. With the same radar parameters, the higher the speed is, the larger the R_L is and the more the integration energy spreads.

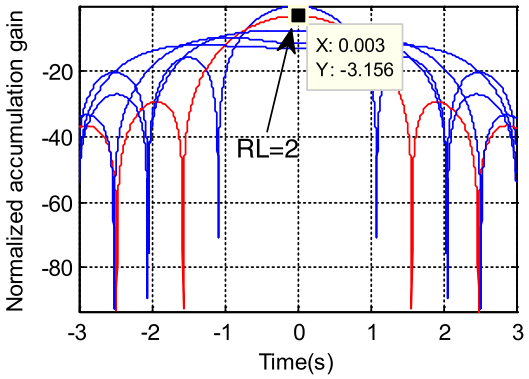

FIGURE 1. Effect of R_L on integration gain.

Figure 1 shows the relation between the target integration gain and the change ratio of SNR_{pulse} as R_L changes. Here, SNR_{pulse} is defined as the integration gain of a single pulse echo signal and can be expressed as:

$$SNR_{pulse} = 10\log_{10}\frac{A_0^2}{\sigma^2} \quad (5)$$

where, A_0 is the target amplitude and σ is the noise power spectral density.

As can be seen from Figure 1, when $R_L \geq 2$, the loss in integration gain is greater than 3 dB. The larger R_L, the greater the loss of integration gains. In order to improve the target detection performance, compensation must be made.

B. STRUCTURE OF RANGE WALK COMPENSATION ALGORITHM

For obtaining a high integration gain, it is necessary to compensate for echo envelope range walk arising from speed. For the sake of processing speed and ease of operation, the algorithms in current use mainly deal with the time domain and frequency domain signals after the echo pulse pressure, and the structure of the compensation algorithms is shown in Figure 2. Among them, the representative method of the frequency domain compensation structure is the keystone transform, and the representative method of the time domain compensation structure is the envelope shift algorithm.

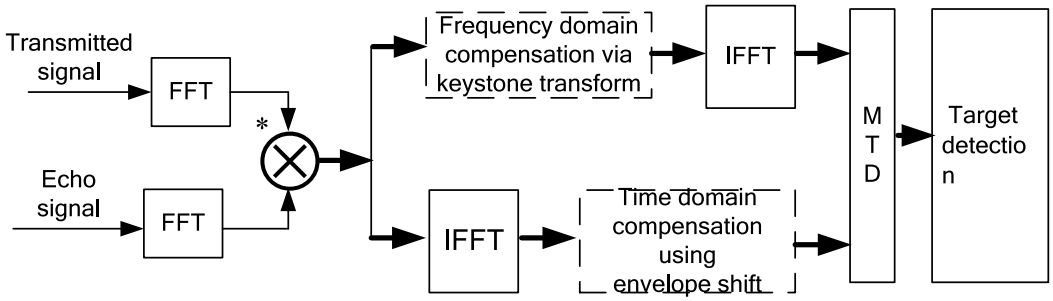

FIGURE 2. Range walk compensation algorithm structure.

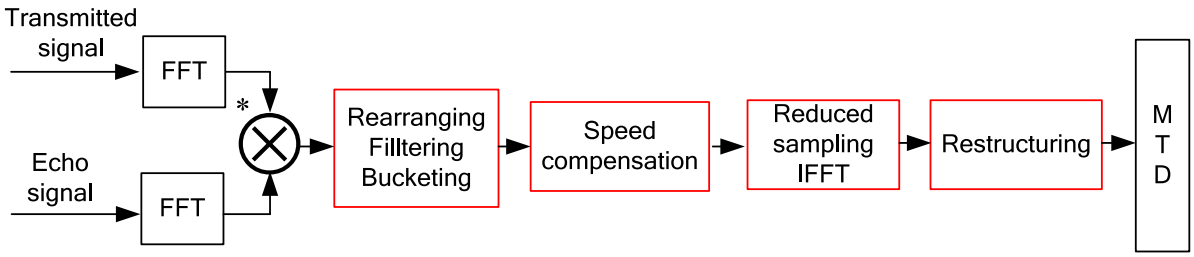

FIGURE 3. Flow diagram of SFT-based range walk compensation method.

The above two structures along with their applications have been studied extensively, but their processing speed is not high and, especially when dealing with long-time, high-speed target signals, the real-time performance is unsatisfactory [25]. To address this problem, this paper, while continuing with the frequency compensation structure, suggests a new method for correcting echo envelope range walk as a means to improve the computational efficiency of the existent methods.

III. SFT-BASED RANGE WALK COMPENSATION METHOD

Based on the frequency domain compensation structure in Figure 2, this paper proposes using the SFT to perform the target speed compensation and range compensation.

According to [12], the frequency domain mathematical model of the n-th echo signal after pulse pressure processing is:

$$X_{(\hat{f},n)} = \frac{A_0}{\sqrt{\mu}}\text{rect}\left(\frac{\hat{f}-f_d/2}{\mu T_0 - f_d}\right)\exp\left(j\pi\frac{2\hat{f}f_d - f_d^2}{\mu}\right) \cdot \exp(j2\pi f_d\,(nT + \tau_0 - \beta_0 nT)) \times \exp(-j2\pi\hat{f}\,(\tau_0 - \beta_0 nT)) \quad (6)$$

The fast time signal spectrum $X_{(\hat{f},n)}$ in (6) is rearranged with the SFT method and is written as $S(m, n)$. Then, there are:

$$S(m,n) = X_{\left(\hat{f},n\right)}\{\hat{f}[(\delta\cdot m) \bmod M], n\}, \quad m \in [1,M], \quad n \in [1,N] \quad (7)$$

where, M is the total number of echo sampling points, N is the number of integration pulses, $\sigma \in [1, M]$ represents the rearrangement factor, with mod N being reversible, and σ and N being coprimes.

In order to extract portions of the signal smoothly and minimize spectral leakage, it is desired to introduce a window function $g(m)$. $g(m)$ should be such that the passband focuses both in the time and frequency domains and that individual sparse large value points can be separated with success. By windowing the rearranged spectrum signal $S(m, n)$, we get:

$$Y(m,n) = g(m)\cdot S(m,n) \quad (8)$$

where, $g(m)$ is as defined in [20]–[22].

Suppose an integer B and it is an aliquot of M, and the following signal is constructed:

$$Z(m,n) = \sum_{i=0}^{\lfloor w/B\rfloor - 1} Y[m + i\cdot B, n], \quad m \in [1,B] \quad (9)$$

where, w represents the time domain window length, B the length after signal grouping. In order that the signal after grouping meets the minimum SNR needed in radar detection, the length of B is defined to be such that:

From the pulse radar detection theory, the SNR produced by aggregate accumulation gain of the pulse pressure processing and the MTD processing should be greater than the minimum detectable SNR $(SNR)_{\min}$ of the target, or

$$10\log_{10}(B) + 10\log_{10}(N) \geq (SNR)_{\min} \quad (10)$$

where, B is the piece length of the number M of sampling points of emission signal, and N is the number of accumulation pulses.

From Equation (10):

$$B \geq 10\text{^}[0.1(SNR)_{\min} - \log_{10} N] \quad (11)$$

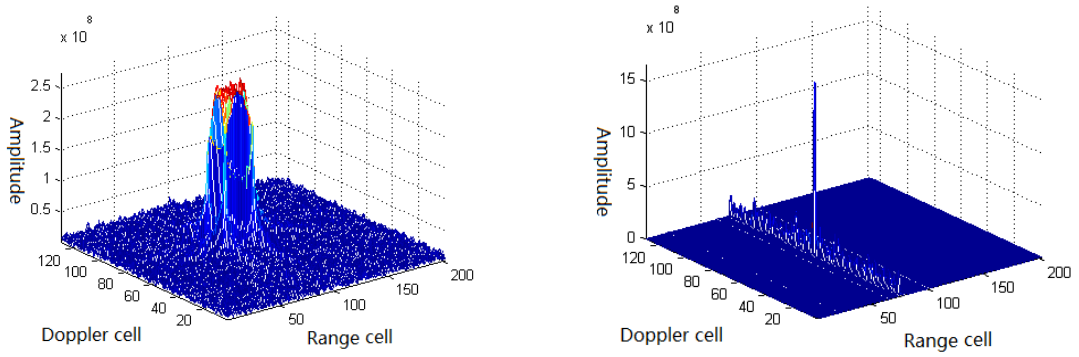

FIGURE 4. Detection results of MTD and the proposed method (speed=1000m/s). (a) MTD, (b) Proposed method.

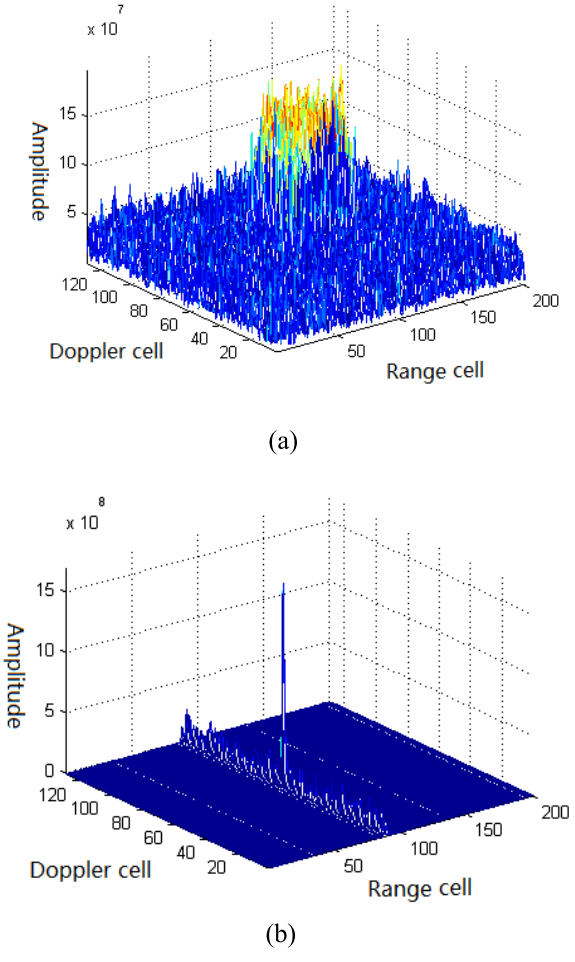

FIGURE 5. Detection results of MTD and the proposed method (speed=2000m/s). (a) MTD, (b) Proposed method.

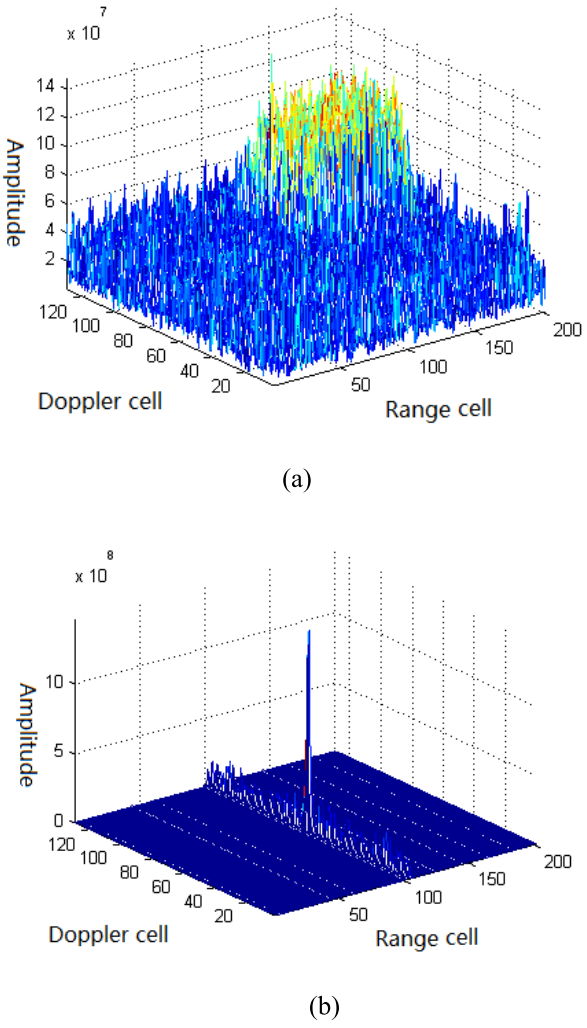

FIGURE 6. Detection results of MTD and the proposed method (speed=3000m/s). (a) MTD, (b) Proposed method.

with

$$(SNR)_{\min} = \frac{\ln P_{fa}}{\ln P_d} - 1 \tag{12}$$

where, P_{fa} is the false alarm probability, P_d is the detection probability, and $(SNR)_{\min}$ is the minimum detection SNR under the condition that P_d and P_{fa} are satisfied.

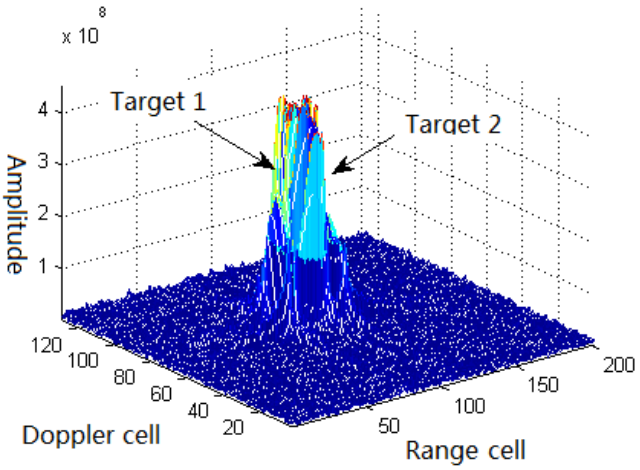

(a)

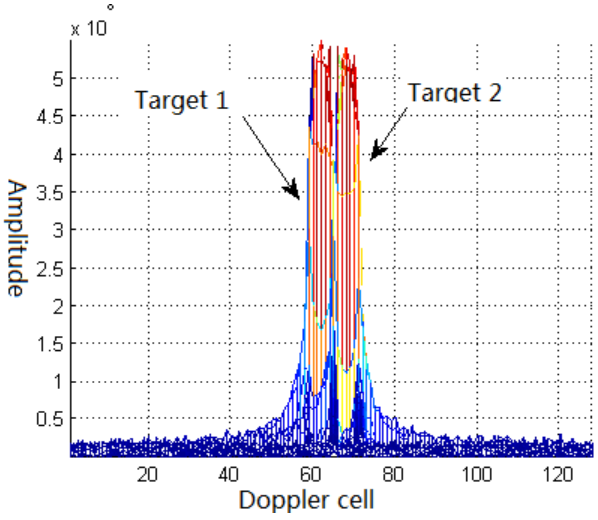

(b)

FIGURE 7. Detection results of two targets by MTD. (a) 3D MTD, (b) 2D projection of MTD.

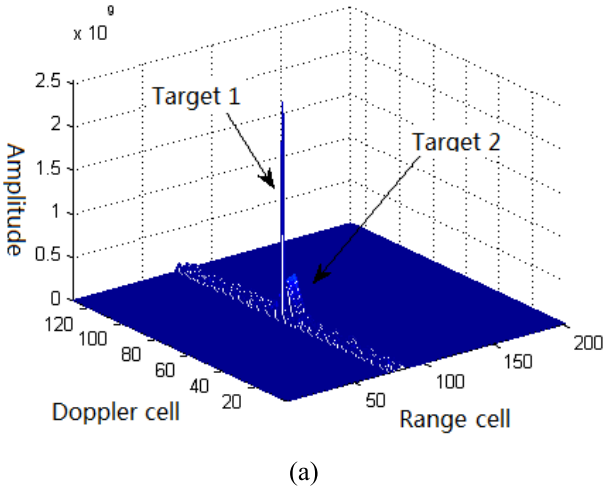

(a)

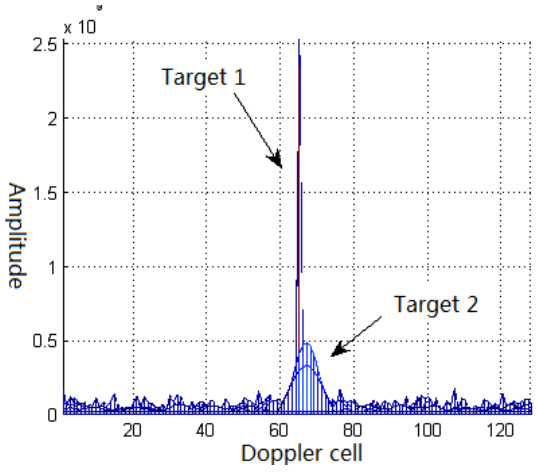

(b)

FIGURE 8. Detection results of two targets by proposed method. (a) 3D result of the proposed algorithm, (b) 2D projection of the proposed algorithm.

Equation (9) converts a long sequence signal into a short sequence one. A speed compensation factor is introduced here to reduce the times of complex multiplication operations. Let the signal after speed compensation be $Z'(m, n)$, then:

$$Z'(m, n) = Z(m, n) \exp[-j2\pi \hat{f} \frac{2\widehat{v}nT}{c}] \tag{13}$$

where, $\widehat{v}$ is the estimate of speed. In actual processing, it can be determined with the help of (5). The range of $\widehat{v}$ can be written as:

$$\begin{aligned} &\hat{v} \in [0, \pm R_L \Delta v, \cdots, \pm PM' \Delta v], \\ &P = round[2BNTv_{\max}/R_L c] \end{aligned} \tag{14}$$

In (14), $v_{\max}$ is the maximum speed of the target. By $R_L \geq 2$, it is suggested that when the range walk exceeds 2 resolution units and the loss of integration gain is greater than 3 dB, speed compensation should be performed before detection.

After speed compensation, IFFT processing of (13) results in:

$$z'(m, n) = IFFT\{Z'(m, n)\} \tag{15}$$

Using the principle in [20], the positioning cycle is performed on $z'(m, n)$. At the end of the estimation cycle, the time domain form of the pulse pressure signal is reconstructed, and the target speed and range are estimated using MTD. Figure 3 presents the flow diagram of the SFT-based range walk compensation method.

IV. PERFORMANCE ANALYSIS

A. ANALYSIS OF TARGET DETECTION PERFORMANCE

1) SINGLE TARGET DETECTION PERFORMANCE

Figures 4–6 compares the performance of MTD and the proposed method when detecting targets of different speeds. The radar and target parameters are listed in Table 1. With the

TABLE 1. Radar and target parameters.

Radar parameters	Carrier frequency	Pulse period	Pulse width	Number of pulses	Bandwidth	Sampling frequency
	3.5GHz	3ms	0.2ms	128	5MHz	10MHz
Target parameters	Range	Initial speed		SNR		
	100Km	1000m/s~3000m/s		-20dB		

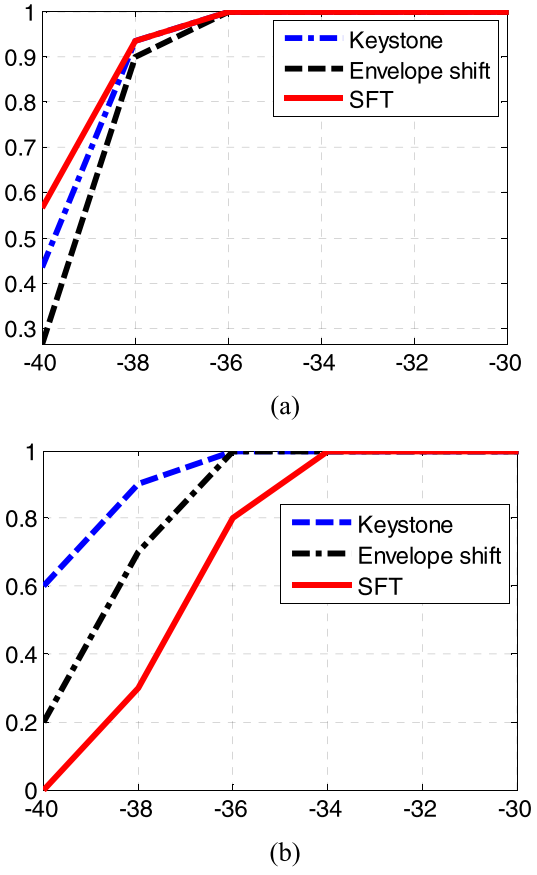

FIGURE 9. Comparison of detection probability of three algorithms. (a) Flat window function, (b) Rectangular window function.

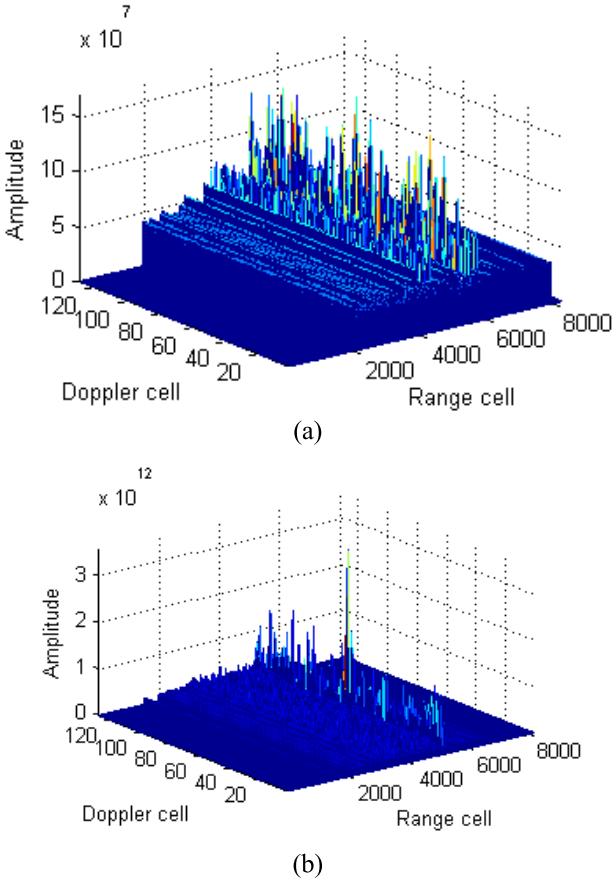

FIGURE 10. Comparison of integration energy when different window functions are used. (a) Flat window function, (b) Rectangular window function.

SFT algorithm, B=1024, the number of positioning cycles is 3, the number of estimation cycles is 8, the degree of sparsity is 2.

Conclusion: As can be seen from Figures 4–6, the proposed method is effective in restraining the spread of integrated energy and yields better integration than MTD, producing an SNR about 10dB higher than MTD.

2) MULTIPLE TARGETS DETECTION PERFORMANCE

The parameters of the radar and the targets are given in Table 1. In this case, the number of targets is 2, with identical amplitude but having a speed of 1000m/s and 1500m/s respectively. Figures 7 and 8 compares the detection performance of MTD and the proposed algorithm. As is obvious in Figure 7, MTD virtually fails to distinguish the two targets while the proposed algorithm fares pretty well. The simulation in Figure 8 includes the detection result of target 1 only, but that of target 2 can be found with CLEAN technique [26].

B. DETECTION PROBABILITY OF DIFFERENT ALGORITHMS

The radar parameters for Figure 9 are given in Table 1. With the SFT algorithm, the signal length is 8192, the signal sparsity is 2, and the number of positioning cycles is 3, the number of estimation cycles is 8, and the noise margin of the filter is 10^{-5}. Figure 9 compares the envelope shift, keystone, and the proposed SFT method. It can be seen that the detection performance of the three is basically the same

when the SNR is high, but when the SNR is low the proposed method has the highest detection probability in Figure 9(a) and the lowest detection probability in Figure 9(b). This is because SFT algorithm uses a different filter function, which produces a different amplitude of segmented signal, affecting the integration energy and the detection probability of the target. In actual use, parameters like the filter window function type and the number of integration pulses shall be adjusted in consideration of the SNR magnitude of the signal and the speed of computation. This will be elaborated in the next section.

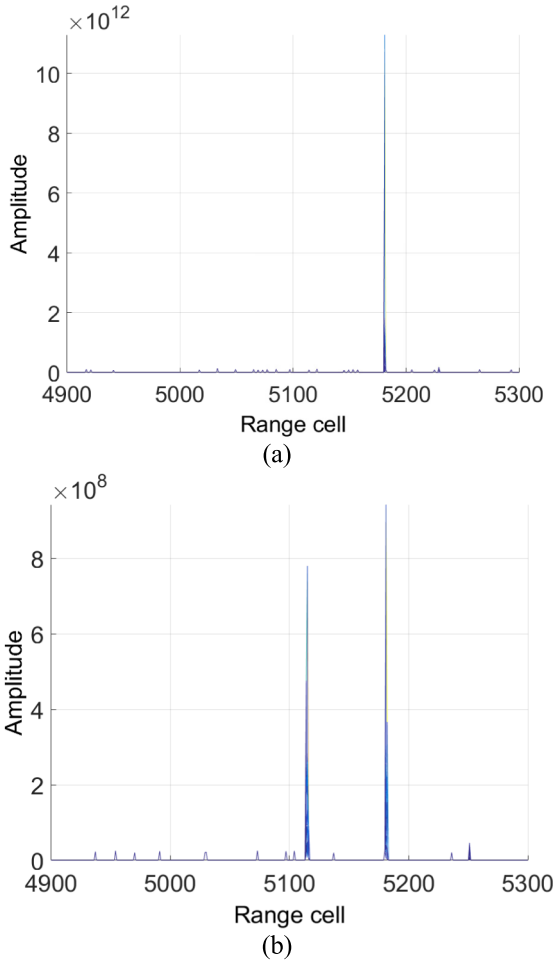

FIGURE 11. Comparison of multi-target resolution for different window functions. (a) Processing result for rectangular window function, (b) Processing result for flat window function.

C. IMPACT OF WINDOW FUNCTION

Figures 10 and 11 compare the detection performance when the window function $g(m)$ is of different types. As shown in Figures 10 and 11, a flat window function in [20]–[22] has advantages of high time-frequency resolution and multi-target resolution capability, a rectangular window function can improve the integration gain of sampled signal, which is

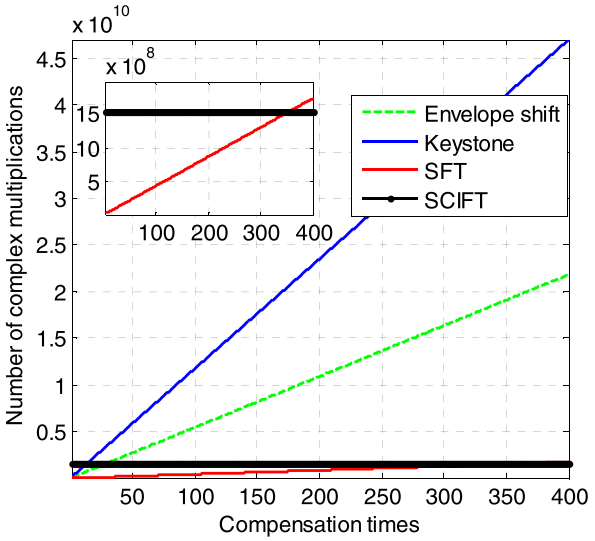

FIGURE 12. Computational complexity comparison of different algorithms with different compensation times.

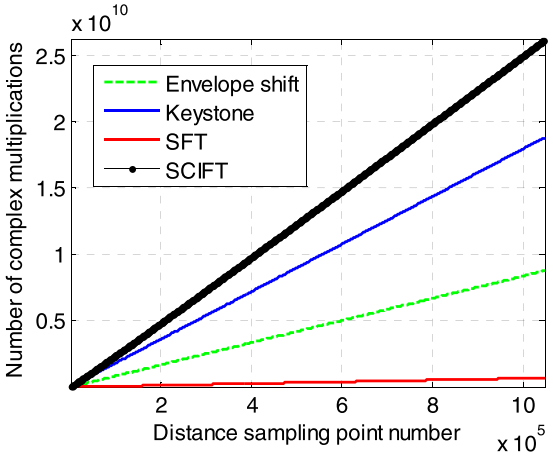

FIGURE 13. Computational complexity comparison of different algorithms with different numbers of range bin sample points.

conducive to the detection of low SNR signals. In practical processing, these two can be used in combination.

D. COMPUTATION LOAD ANALYSIS

Let M, N, and L be the number of sampling points in the pulse gate, the number of integration pulses, and the number of speed compensation channels, respectively. If the envelope interpolation algorithm in [12] is adopted, the number of complex multiplication operations needed for L searches is $(3/2)M\log_2(M) + L[3MN + (MN/2)\log_2(N)]$. As for keystone-based method suggested in [11], the number of complex multiplication operations required for L searches is $L[2MN\log_2 N + 3N(\log_2 N)/2]$. The SCIFT algorithm proposed in [16] involves $MN^2 + 3MN\log_2 M + MN\log_2 N$ complex multiplication operations. With the SFT-based algorithm proposed in this paper, the window length is set to w, the bucket length is B, k is the sparsity, l_{loc} is the number of

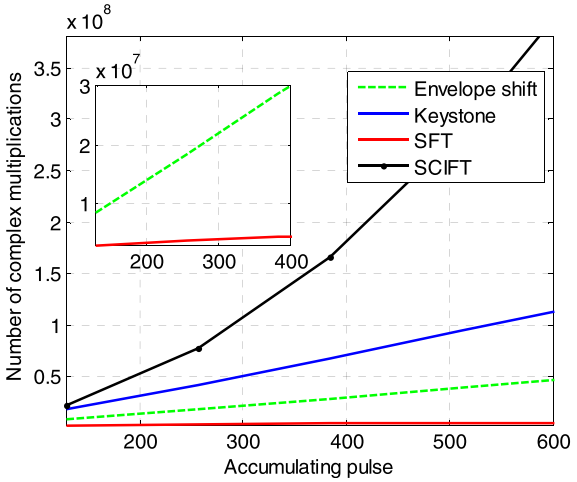

FIGURE 14. Computational complexity comparison of different algorithms with different accumulate pulse numbers.

positioning cycles, l_{est} is number of estimation cycles, and l_{total} is the number of total cycles. For one speed compensation operation, the number of complex multiplications is $(M+1)\log_2(M)+(B+y_{sft})+(NM/2\log_2 N)$. For one SFT operation of M points, complex multiplications of order $y_{sft}=(w+B\log_2 B/2)\times l_{loc}+(B\log_2 B/2)\times l_{est}+2kM/B\times l_{total}$ are needed, and L searches need $M\log_2(M)+L[(B+y_{sft})+(0.5NM\log_2 N)]$ of complex multiplications. The simulation parameters are given in Table 1. Figure 12 compares the computation load of the four algorithms with different L. It can be observed that, when $L<300$, the computation load of the proposed SFT algorithm is lower than that of the other three algorithms. When $L>300$, the proposed SFT algorithm has a computation load higher than that of the SCIFT method in [16] and [17]. Figures 13 and 14 compare the amounts of complex multiplication with the four algorithms for L=50 when M is in the range $[2^{10}, 2^{20}]$, and N in the range [128, 2048]. Among these four methods, the SFT algorithm has the lowest computational load and SCIFT has the highest. This is because the computational load of the SCIFT algorithm approximates to MN^2. Here, L is smaller, because in practical target detection scenarios, certain *a priori* information can be obtained in advance. As such, an approximate speed range can be estimated.

V. CONCLUSION

Long time integration of weak high-speed targets generally causes range walk, i.e., energy dispersion across range bins. In this paper, we analyze the key factors that influence range walk and propose a high-speed target detection algorithm based on SFT, which is advantageous over various existing range walk compensation methods in terms of computational efficiency. As known from the theories and simulation described in this paper, the proposed method is quick in processing long-range and high sampling rate signals. Relative to existing methods, it performs speed compensation of long sequence signal by advantageously converting the signal into short sequence signal, which further minimizes the times of complex multiplications and thus improves the algorithm efficiency. The simulation results also indicate that the selection of window function has impact on the target resolution and detection performance. Our further research will focus on resolving multiple targets with the proposed method in a lower SNR condition.

REFERENCES

[1] E. J. Kelly and R. P. Wishner, "Matched-filter theory for high-velocity, accelerating targets," *IEEE Trans. Mil. Electron.*, vol. MIL-9, no. 1, pp. 56–69, Jan. 1965.
[2] D. Orlando, L. Venturino, M. Lops, and G. Ricci, "Track-before-detect strategies for STAP radars," *IEEE Trans. Signal Process.*, vol. 58, no. 2, pp. 933–938, Feb. 2010.
[3] J. Carretero-Moya, J. Gismero-Menoyo, A. Asensio-Lopez, and A. Blanco-del-Campo, "Application of the radon transform to detect small-targets in sea clutter," *IET Radar Sonar Navigat.*, vol. 3, no. 2, pp. 155–166, Apr. 2009.
[4] J. Xu, X.-G. Xia, S.-B. Peng, J. Yu, Y.-N. Peng, and L.-C. Qian, "Radar maneuvering target motion estimation based on generalized radon-Fourier transform," *IEEE Trans. Signal Process.*, vol. 60, no. 12, pp. 6190–6201, Dec. 2012.
[5] J. Xu, J. Yu, Y.-N. Peng, and X.-G. Xia, "Radon-Fourier transform for radar target detection, I: Generalized Doppler filter bank," *IEEE Trans. Aerosp. Electron. Syst.*, vol. 47, no. 2, pp. 1186–1202, Apr. 2011.
[6] J. Xu, J. Yu, Y.-N. Peng, and X.-G. Xia, "Radon-Fourier transform for radar target detection (II): Blind speed sidelobe suppression," *IEEE Trans. Aerosp. Electron. Syst.*, vol. 47, no. 4, pp. 2473–2489, Oct. 2011.
[7] T. J. Abatzoglou and G. O. Gheen, "Range, radial velocity, and acceleration MLE using radar LFM pulse train," *IEEE Trans. Aerosp. Electron. Syst.*, vol. 34, no. 4, pp. 1070–1083, Oct. 1998.
[8] Z. Jiankui, H. Zishu, M. Sellathurai, and L. Hongming, "Modified Hough transform for searching radar detection," *IEEE Geosci. Remote Sens. Lett.*, vol. 5, no. 4, pp. 683–686, Oct. 2008.
[9] T. Shan, S. Liu, Y. D. Zhang, M. G. Amin, R. Tao, and Y. Feng, "Efficient architecture and hardware implementation of coherent integration processor for digital video broadcast-based passive bistatic radar," *IET Radar Sonar Navigat.*, vol. 10, no. 1, pp. 97–106, Jan. 2016.
[10] G. Sun, M. Xing, X.-G. Xia, Y. Wu, and Z. Bao, "Robust ground moving-target imaging using deramp–keystone processing," *IEEE Trans. Geosci. Remote Sens.*, vol. 51, no. 2, pp. 966–982, Feb. 2013.
[11] X. Lv, M. Xing, C. Wan, and S. Zhang, "ISAR imaging of maneuvering targets based on the range centroid Doppler technique," *IEEE Trans. Image Process.*, vol. 19, no. 1, pp. 141–153, Jan. 2010.
[12] P. C. Suo, S. Tao, R. Tao, and Z. Nan, "Detection of high-speed and accelerated target based on the linear frequency modulation radar," *IET Radar Sonar Navigat.*, vol. 8, no. 1, pp. 37–47, Jan. 2014.
[13] Y. Wang and Y. Lin, "ISAR imaging of non-uniformly rotating target via range-instantaneous-Doppler-derivatives algorithm," *IEEE J. Sel. Topics Appl. Earth Observ. Remote Sens.*, vol. 7, no. 1, pp. 167–176, Jan. 2014.
[14] J. Zhang, T. Su, J. Zheng, and X. He, "Novel fast coherent detection algorithm for radar maneuvering target with jerk motion," *IEEE J. Sel. Topics Appl. Earth Observ. Remote Sens.*, vol. 10, no. 5, pp. 1792–1803, May 2017.
[15] A. S. Paulus, W. L. Melvin, and D. B. Williams, "Multichannel GMTI techniques to enhance integration of temporal signal energy for improved target detection," *IET Radar Sonar Navigat.*, vol. 11, no. 3, pp. 395–403, Mar. 2017.
[16] J. Zheng, T. Su, W. Zhu, X. He, and Q. H. Liu, "Radar high-speed target detection based on the scaled inverse Fourier transform," *IEEE J. Sel. Topics Appl. Earth Observ. Remote Sens.*, vol. 8, no. 3, pp. 1108–1119, Mar. 2015.
[17] J. Zheng, T. Su, H. Liu, G. Liao, Z. Liu, and Q. H. Liu, "Radar high-speed target detection based on the frequency-domain deramp-keystone transform," *IEEE J. Sel. Topics Appl. Earth Observ. Remote Sens.*, vol. 9, no. 1, pp. 285–294, Jan. 2016.
[18] X. Chen, X. Yu, J. Guan, and Y. He, "An effective and efficient long-time coherent integration method for highly maneuvering radar target in sparse domain," in *Proc. 4th Int. Workshop Compressed Sens. Theory Appl. Radar Sonar Remote Sens.*, Sep. 2016, pp. 124–127.

[19] J. Wen, D. Li, and F. Zhu, "Stable recovery of sparse signals via l_p-minimization," *Appl. Comput. Harmon. Anal.*, vol. 38, no. 1, pp. 161–176, Jan. 2015.
[20] J. Wen, J. Wang, and Q. Zhang, "Nearly optimal bounds for orthogonal least squares," *IEEE Trans. Signal Process.*, vol. 65, no. 20, pp. 5347–5356, Oct. 2017.
[21] H. Hassanieh, P. Indyk, D. Katabi, and E. Price, "Nearly optimal sparse Fourier transform," in *Proc. 44th Annu. ACM Symp. Theory Comput.*, May 2012, pp. 563–578.
[22] J. Wen, Z. Zhou, J. Wang, X. Tang, and Q. Mo, "A sharp condition for exact support recovery with orthogonal matching pursuit," *IEEE Trans. Signal Process.*, vol. 65, no. 6, pp. 1370–1382, Mar. 2017.
[23] S. Liu, Y. D. Zhang, and T. Shan, "Detection of weak astronomical signals with frequency-hopping interference suppression," *Digit. Signal Process.*, vol. 72, pp. 1–8, Jan. 2018.
[24] S. Liu *et al.*, "Sparse discrete fractional Fourier transform and its applications," *IEEE Trans. Signal Process.*, vol. 62, no. 24, pp. 6582–6595, Dec. 2014.
[25] D. Wang, C. Lin, Q. Bao, and Z. Chen, "Long-time coherent integration method for high-speed target detection using frequency agile radar," *Electron. Lett.*, vol. 52, no. 11, pp. 960–962, May 2016.
[26] X. Li, L. Kong, G. Cui, and W. Yi, "CLEAN-based coherent integration method for high-speed multi-targets detection," *IET Radar Sonar Navigat.*, vol. 10, no. 9, pp. 1671–1682, Dec. 2016.

CUNSUO PANG received the Ph.D. degree in electronics engineering from the School of Information and Electronics, Beijing Institute of Technology, China, in 2014. He is currently a Lecturer with the School of Information and Communication Engineering, North University of China. His research interests include radar signal processing and time-frequency analyses.

SHENGHENG LIU received the B.Eng. and Ph.D. degrees in electronics engineering from the School of Information and Electronics, Beijing Institute of Technology, China, in 2010 and 2017, respectively. He was a Visiting Research Associate with the Department of Electrical and Computer Engineering, Temple University, Philadelphia, PA, USA, from 2015 to 2016, under the support of the China Scholarship Council. He is currently a Post-Doctoral Fellow with the Institute for Digital Communications, School of Engineering, The University of Edinburgh, U.K. His research interests include compressive sensing and time-frequency analyses for non-stationary signals, interference canbination and coherent integration for passive bistatic radars, and image reconstruction in electrical impedance tomography. He is a frequent reviewer for several top-tier journals, including the IEEE TRANSACTIONS ON SIGNAL PROCESSING, the IEEE TRANSACTIONS ON AUDIO, SPEECH, AND LANGUAGE PROCESSING, and the IEEE TRANSACTIONS ON INSTRUMENTATION AND MEASUREMENT.

YAN HAN received the Ph.D. degree from the Beijing Institute of Technology, China, in 1998. He is currently a Professor of signal and information processing with the School of Information and Communication Engineering, North University of China. His main research interests include signal and information processing, non-destructive detection, and sensor networks.